

# ATD: Design and Construction of the Autonomous Test Driver

Ryan Stevens  
MAEB 325, UF  
4995 SW 14<sup>th</sup> PI #822B  
Gainesville, FL, 32607  
stevrt@ufl.edu

Eric M. Schwartz  
MAEB 321  
University of Florida  
Gainesville FL 32611  
ems@mil.ufl.edu

A. Antonio Arroyo  
MAEB 338  
University of Florida  
Gainesville FL 32611  
arroyo@mil.ufl.edu

## ABSTRACT

The following report outlines the design guidelines associated with ATD: The Autonomous Test Driver. ATD's design allows it to quickly navigate a walled course, utilizing fast integrated sensors to accurately detect the course and to a rudimentary job in learning to navigate the course. After a slow first traversal of a course, when ATD learns the required sequence and locations of turns, on subsequent loops around the track, he will drive the course aggressively, attempting to complete it as quickly as possible. ATD was by an Atmega128 microcontroller integrated with an small array of commercial rangefinders in order to avoid the track walls and a gyroscope to record information about the course turns. Crude course mapping and a slight speed increase were implemented. ATD also utilized LCD and LED for debugging feedback and for demonstration purposes.

## Keywords

Robotics, Automobile, Sensor Fusion, Mapping

## 1. INTRODUCTION

As automobile manufacturers strive for vehicles that maintain both high performance and exceptional fuel economy, the requirements of automotive testing become more and more stringent. With component and system complexity ever increasing, the probability of an individual failure impacting the overall vehicle performance is increased as well. To aid manufacturers in the testing of these vehicles, an autonomous test driving (ATD) system would allow the manufacturer to test vehicles on various track designs without risking human life in an accident. An ATD would also allow the vehicle to be driven repeatedly to its precise limitations in order to assess component wear and vehicle performance.

A small autonomous car, appropriately named ATD, was constructed to meet these objectives. ATD drives around a walled course, and attempts to navigate around this course as quickly as possible. This robot provides a small-scale solution to car testing problem, and will also lays the groundwork for a possible full-scale robotic platform in the future. The following documentation outlines the specifications and design of ATD: the Autonomous Test Driver.

## 2. INTEGRATED SYSTEM

ATD was originally designed to consist of a variety of sensors, electronics, and motors connected to a central microcontroller board. These components were integrated via device drivers in software and high-level arbitration subroutines that govern the

logic and intelligence of the robot. Figure 1, shown on the next page, details the components and interface bus layout of the electrical system as originally specified.

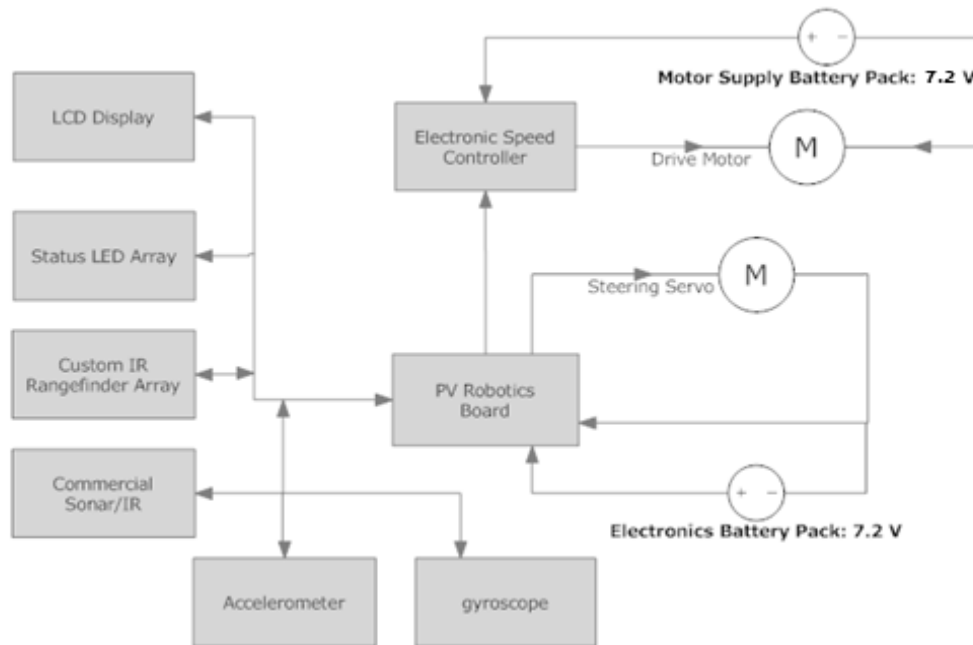
The PV Robotics [1] board serves as the main controller for the entire autonomous platform. The Atmega128 microcontroller on this board receives sensory inputs, outputs motor control signals, and drives the LCD and LED displays. The ATmega128 processes all AI algorithms and controls the autonomous vehicle throughout its operation. The board makes use of its extensive memory to record basic data gained from the sensors, and stores calibration data obtained during the vehicle's startup calibration sequence.



Figure 1: PV Robotics Controller Board

The LCD display is a GDM1602K from Sparkfun Electronics. The LCD screen is used to provide text feedback during calibration and testing of the robotic platform. The LED array consists of three LEDs (red, yellow, and green) which indicate operating modes, and serve as sensor indicators. As the vehicle steers, two of the LEDs indicate which direction it is attempting to steer. As it crosses the lap marker, all three LEDs light up to indicate completion of a lap. Due to issues with software overhead, during the driving phase, the LCDs are not used since they effectively slow down the control loop.

The primary sensor system was intended to be an array of individually tuned IR rangefinder emitter/detector pairs. Each sensor would receive IR reflections of a transmitted square wave at a specific tuned frequency. The intensity of this reflection indicates the relative distance from the reflecting surface. Each element of the array was to contain additional circuitry to filter and interface the sensor outputs to the microcontroller. This sensor would have been used to visualize the course ahead of the robot, as the driving algorithm will require a high amount of sensory data to properly maneuver the course. Due to issues with construction, this sensor was not completed. The analog circuitry



**Figure 2: Integrated System**

worked as expected, but coupled noise from an unknown source on the receiver board effectively negated effective operation. The circuitry was thus abandoned near the end of the semester in favor of using successfully operating sensors to accomplish the same behaviors, but with reduced capability.

For wall-following and rear obstacle avoidance, commercial Sharp IR GPD12DY rangefinders [2] are used in pairs on both sides of the robot. This arrangement will allow the vehicle to precisely align parallel to a wall, and allow it to drift closer or farther from a specific wall. These sensors are used to avoid side obstacles. Due to issues with the primary IR array, these sensors also serve as the primary sensors for determining steering directions for the robot.

The servo and drive motors serve to maneuver the robot around the field. The servo motor is a standard R/C hobby servo, and controls the Ackermann steering mechanism of the car chassis. The DC drive motor applies power to the rear wheels and is controlled via the electronic speed controller (ESC). The ESC is a hobbyist digital-proportional motor controller that is controlled by outputs from the microcontroller. It applies the proper voltages to the drive motor to operate at various speeds.

The accelerometer is a MEMS device that is used to provide PID feedback control for the robot. Rather than use a shaft encoder, the motor control feedback is based on the positive or negative acceleration detected by the accelerometer. This would allow the autonomous agent to accelerate or decelerate precisely. The gyroscope allows the vehicle to record the sequence and relative angle of each turn on the course [3]. Experimental testing of the accelerometer indicated that vibration from the motor provides a source of noise. As a result, both of these sensors are filtered by running average filters implemented by the ATmega128. While this smoothed the gyro output, it did not fully stabilize the accelerometer, and the negligible enhancement to operation resulted in a complete removal of the accelerometer from the

software system. Both of these devices were connected to the PV Robotics board utilizing an SPI enabled MAX1113 ADC chip [4].

The power distribution system consists of two separate battery packs. The main drive motor battery pack is a 7.2V NiMH battery pack used solely to drive the main DC Motor. The second battery pack is a 7.2V NiMH battery pack which provides the power for the steering servo and the main electronics package. Two on/off switches allow either of these supplies to be independently activated. One of these switches is mounted on the ESC, while the other is directly mounted on the wooden superstructure.

In addition to these devices, a CdS cell and LED illuminator were added to detect the presence of a starting strip, implemented with black strip of tape along the ground. The CdS cell was connected via a simple voltage divider into one of the ports on the MAX1113 ADC originally used for the accelerometer. Utilization of this sensor allowed the robot to detect when it had completed a lap, as well as allowing ATD to detect two strips of tape in rapid succession and use this condition as a stop trigger.

### 3. MOBILE PLATFORM

The design of a curving, winding test track present special difficulties in mechanical platform design. The vehicle must be able to turn precisely while driving forwards, and be able to perform both small and large turns without having to resort to stopping to complete the maneuver accurately. Utilizing a platform with the same mechanical design as a modern automobile would satisfy these requirements and allow the electronics and mathematics of the robot to be directly scalable to a full size vehicle.

In order to fulfill these requirements, the mobile platform consists of a 1/18<sup>th</sup> scale R/C Car Chassis, the Team LOSI Mini-T. This chassis contains spring suspension, an Ackermann steering mechanism, and a rear-wheel differential drive train. These mechanical systems allow the platform to maneuver as a real car

maneuvers, and allows it to brake, accelerate, and turn simultaneously in a smooth fashion. This mechanical platform provides the best solution to the kinematic challenges of driving a winding course at high speed.

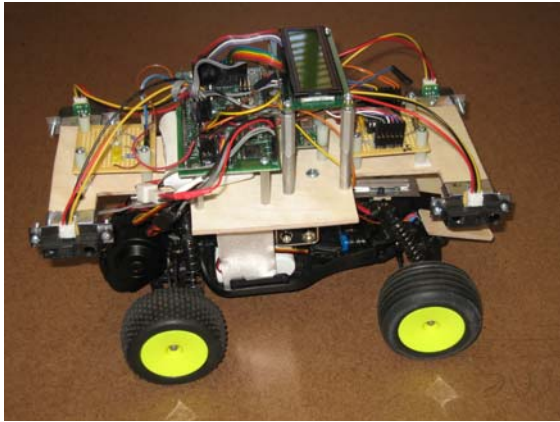


**Figure 3: Assembled Robotic Platform**

Furthermore, the mechanical platform contains a wooden superstructure attached to the four latch-pin posts on the Mini-T chassis. This portion of the chassis is built of sheet metal, and reinforced with a supporting bracket that fits underneath the drive motor battery pack on the car chassis, and provides additional vertical support. The ATmega128 board, LCD screen, accelerometer/gyroscope, and Sharp IR rangefinders are mounted on the superstructure. The CdS cell and illumination LED were added to the main chassis of the robot, with a small wooden board on top of the two to reduce the effects of ambient lighting on the cell.

#### **4. ACTUATION**

ATD contains two main actuators: the steering system, and the drive-train. These two actuations must work in concert together to accelerate in a straight line, maneuver through a turn, and avoid obstacles. The steering linkage is actuated by a small R/C servo, an HS-55, which was installed in place of the original 4 wire servo, which lacks control circuitry. The drive-train is powered by a small DC motor which was pre-installed in the chassis.

The steering mechanism is an Ackermann steering linkage. In this type of steering, the servo rotates to slide a direct linkage which is connected to the front wheels themselves. This rotates the front wheel mounts to allow the vehicle to turn either left or right. The amount of servo rotation affects the turning radius of the vehicle at any given moment. However, this type of steering mechanism is constrained in that it is dependent upon forward or reverse motion of the vehicle itself. As a result, turns must be initiated with some non-zero vehicle velocity. Further complicating the steering, the velocity of the vehicle has some impact on the turning radius as well.

As a result of these complexities, the servo will be controlled by PWM output from the microcontroller via a turning arbitration subroutine. This subroutine will ensure that proper velocity is maintained when entering and exiting the turn via communication with the rear-wheel drive control subroutine. Output of the PWM signal will adjust the servo's position, and allow for very precise control of ATD [1].

The rear-wheel drive system is the second actuator present on ATD. This drive-train links the output of the DC motor to a series of gears, a slipper clutch, and a rear-wheel differential and its associated output shafts. This mechanical system serves to allow the motor to apply torque and accelerate the vehicle while allowing the individual rear wheels to turn at different angular velocities. This arrangement minimizes slip during turns, and ensures that all four wheels will maintain grip on the driving surface during most maneuvers. While braking via driving the motor in reverse was considered, it was not necessary at the operational speeds and scale of ATD. To decelerate, simply leaving the motor at zero power will allow ATD to come to a quick stop. This was experimentally verified using the remote control system that came with the Mini-T. As a result, all actuation of the drive-train will be controlled via the PV Robotics board, which will send control signals to the ESC to accelerate the motor or let the robot coast to a stop. While a PD controller involving the accelerometer was considered, uncontrollable noise on the accelerometer due to motor vibration, and the stability of the ESC negated its requirement in the overall control system.

#### **5. SENSORS**

The sensor suite of ATD was specifically designed to utilize the optimum sensors for each sensing task. As the robot will travel short distances at higher speeds, typical data acquisition rates must be higher than 10 Hz. As a result, data is evaluated in a decision making process at nearly 40 Hz to allow the vehicle to respond rapidly. The designed rangefinder array will not be discussed here, as it was not fully implemented on the robot.

The side Sharp GP2D120 short range IR rangefinders serve to detect the side walls of the course. Experimental testing determined that the Sharp IR rangefinders exhibited superior short range performance compared to sonar systems. These sensors are mounted on either side of the wooden superstructure, and are run straight into the ADC channels on the PVRobotics board [1]. Experimental results show that the system allows for good wall-following at low speeds, but at higher speeds, ATD must begin turning before drastic wall changes, especially if the course width is narrow, and thus the distance between the wall and the robot small. However, using the difference between each sensor allows the robot to easily and precisely align parallel to a wall with minimal programming overhead. Furthermore, weighting the steering input with the front two IR values provides a more stable response, and prevents the robot from accidentally hitting the walls in certain track conditions.

An accelerometer was originally to be used to implement feedback for acceleration control in the autonomous platform. Ideal sensitivity is approximately 1 g for full swing of the output voltage. This provides maximum resolution as the vehicle is unable to accelerate this quickly. The Analog Devices ADXL203 was selected for this role as part of a combo board with the ADXRS401 gyroscope offered by Sparkfun Electronics [3]. However, motor mount vibration made this sensor extremely noisy, and running average filtering was unable to fully compensate for this effect. Furthermore, the ESC proved to be effective on its own, and so the accelerometer based feedback was eliminated from the project.

The gyroscope serves a critical role in the sensor suite of ATD. The gyroscope's primary purpose is to record angular change

during the initial lap of the course. This data will allow ATD to record the sequence of “soft” and “hard” turns that comprise the course. With this knowledge, ATD will be capable of modifying its route on successive laps to better drive the course quickly. The ADXRS401 gyroscope from Analog Devices proved to be a successful gyroscope for this application. Running average filtering was implemented in software, and thresholds were used to determine which turn ATD was making at any instant [3].

The CdS cell was added to detect the lap marker and to identify a set of black lines to indicate a request to stop ATD. It was wired up with a voltage divider, and placed at the base of the robot. As the robot drives around the course, it is able to detect the lap marker with a high degree of accuracy.

The CdS cell, and gyroscope are interfaced with a SPI enabled MAX1113 ADC from Maxim IC. This system acquires the data at 1000 Hz and implements eighth order running average filtering on the gyroscope [4]. All other sensor data is acquired at 40 Hz using a data acquisition clock onboard the PV Robotics board. This data rate was chosen as it sits approximately at the response time of the Sharp IR Rangefinders [2].

## 6. BEHAVIORS

There are three main behaviors associated with ATD’s tasks. The first and primary task is the drive algorithm. This algorithm interprets data from the side sensor arrays to avoid walls and navigate the turns of the course. Drive motor control is accomplished through another subroutine that sets the PWM control for the ESC to a specified percentage of full power.

The steer algorithm is constantly computing a weighted summation of the forward two sharp IR rangefinders and the differences between the left and right Sharp IR rangefinder pairs. Inspiration for this type of algorithm came from artificial neurons, in which weighted summations map inputs to outputs. Simplification of the mathematics of the weighting was done by using bit-shift operators to reduce the influence of specific terms, rather than using floating point math which would increase software overhead. This weighted summation drives the steering servo through a steer subroutine that accounts for the mechanical limits of the servo mount. This subroutine is running continuously in the main operation loop and constantly updates the servo position accurately.

The second behavior is the initial lap drive, which is initiated at startup. Following calibration of the sensors, ATD will begin driving the course. As the robot slowly navigates the course, this behavior will identify and record the sequence of the first ten turns the robot completes. Following completion of this lap, the behavior will hand off arbitration of the robot to the second high level navigation behavior.

The second main navigation arbitration behavior is the speed lap driving algorithm. In this algorithm, due to time and programming constraints, the speed of the drive system was the only noticeable feature increased. An attempt to utilize gyro acquired turn data to improve turning was pursued but was unable to be completed in time. As a result, the robot improves its speed marginally on the subsequent laps. The course size, being exceptionally small, however, limits this speed increases severely.

In addition, a stop behavior was added to ATD. If ATD detects two black tape markers within a short period of time, it will turn its motor off, and coast to a stop. Following this, it will print out

the sequence of turns it recorded in the first lap. Currently, the sequence is capped at the first 10 turns, though this is acceptable for the current course sizes used in demonstrations. This behavior works excellently, and allows an observer to easily stop ATD by simply quickly laying down another piece of tape near the lap marker. This also allows for a demonstration of a discontinuous track which better displays ATD’s capability to map the first ten turns of a course.

## 7. EXPERIMENTAL RESULTS

Experiments were performed to determine the speeds at which ATD was to operate during demonstrations. The following qualitative assessments were made:

**Table 1: Drive Speed Evaluation Results**

Speed Value	Evaluation
15	Moderately fast, stable on small courses
16	Faster, slightly less stable, occasionally fails on small courses
>= 17	Extremely unstable.

As a result, ATD was programmed to drive at 14% power during the initial slow lap and 15% during the faster lap. Due to the nature of the ESC controller at lower power ratings, this speed increase is actually far more significant than the 1% indicates, as the response is non-linear.

As well, the CdS cell thresholds were determined for both the UF New Engineering Building (NEB) and for Benton Hall. At Benton hall, a value of -40 was sufficient for operation, due to the white floor. However, at NEB, the multicolor floor presented a problem. The black tile appeared so close to the black tape, and the differences in values between black tape on black tile, and black tape on white tile, forced a modification to the track. The CdS value was set at -25, and the black tile was covered with white poster board and white printer paper. This was the only option as no sufficient threshold could be determined for the case of all three types of tile. However, ATD works perfectly over the burgundy and white tiles, and still displays robust operation over a wide operating environment. In the case of NEB, a very specific and non-ideal case presented itself that could not be compensated for in software or hardware without field modifications.

During testing on the walled track, it was determined that a white coat of paint to each block would significantly improve IR reflectivity. After this track change was implemented, ATD’s performance around the turns at slower speeds became very consistent. However, the course layout must be carefully designed, as with the limited wood available only a very tight, very compact course can be built. As a result, for ATD to complete the course effectively, some amount of course engineering must be employed when laying out the track, as ATD can simply not turn hard enough to execute turns within a certain turning radius.

## 8. CONCLUSION

The design proposal described above laid a solid foundation for the initial design of an autonomous test track driver. The ATD project provided the opportunity to develop a robust robotic platform capable of driving a complex course quickly. This not

only provided a proof of concept for autonomous driving agents, but also developed a scaled prototype of what could be developed into a full-scale autonomous driving system for a modern automobile.

ATD realistically accomplishes partial functionality of its original intended goals. It can drive around a closed course, increase its speed marginally, and establish crude turn mapping whilst driving. However, it is not exceptionally fast, nor does it make use of a custom IR rangefinder array. Despite these limitations, it does manage to establish a strong proof of concept of an autonomous test-track robotic platform.

The usages of commercial Sharp IR rangefinders exceeded initial expectations, and were able to effectively resolve drive inputs for ATD at moderate speeds. Had more time been allotted, and the special sensor fully debugged and operational, these capabilities would have been capable of implementing more advanced driving.

Future work in this area of robotics should focus on continued development of advanced, high capability IR sensors that, if successful, offer significant improvements in terms of course detection and resolution. As well, specifications for motor control systems will need to be revised, as accelerometer based feedback turned out to be marginally useful, and noise in this system was extremely difficult to overcome. Furthermore, emphasis on larger course designs that approximate scale models of actual race tracks would significantly improve testing and performance, as the current track options are simply too small to allow effective operation of a 1/18<sup>th</sup> scale car. Methods of artificial neuron training via analysis of human control offer the possibility of significantly improved drive software algorithms as well, and should also be investigated.



Figure 4: ATD within the wooden walled course

## 9. ACKNOWLEDGMENTS

My thanks to Dr. Arroyo and Dr. Schwartz for offering students an exciting and interactive learning environment.

## 10. REFERENCES

- [1] Pridgen, M. Vermeer, T. *Pridgen Vermeer Robotics ATmega128 Revision 0*. [http://www.mil.ufl.edu/imdl/handouts/PV\\_Rob\\_Manual\\_R0.pdf](http://www.mil.ufl.edu/imdl/handouts/PV_Rob_Manual_R0.pdf).
- [2] Sharp Optoelectronic Devices Division. *GPD2D120XJ100F Specification*.
- [3] Sparkfun Electronics. *ADXL203/ADXRS401 IMU Board Datasheet*. <http://www.sparkfun.com>. 2005.
- [4] Maxim IC. *MAX1112/1113 Datasheet*. October, 1998.